

Pyridinium salts and ylides as partial structures of photoresponsive Merrifield resins

Marcel Albrecht,^a Maxim Yulikov,^c Thomas Kohn,^c Gunnar Jeschke,^c Jörg Adams^b and Andreas Schmidt^{*a}

Received 23rd September 2009, Accepted 28th January 2010

First published as an Advance Article on the web 26th February 2010

DOI: 10.1039/b919862h

Merrifield resin was treated with 4,4'-bipyridine and 2,4'-bipyridine, respectively, to give photochromic materials. On exposure to light, reversible color changes are observable. These resins also serve as indicators because reversible color changes are observable on addition of bases, which deprotonate the benzylic position of the *N*-benzylpyridinium salts to ylides. These can be detected spectroscopically and by trapping reactions on monomeric model compounds. EPR and HYSCORE measurements in combination with DFT calculations prove that radical species are formed in either case. Evidence is found that the carbanionic centers of the ylide partial structures serve as electron donors in these reversible color changes, thus setting them apart from known photochromic materials.

Introduction

The applications of photochromic materials can be divided into two categories, which are based on (i) changes of the absorption or emission spectra, or (ii) changes of other chemical and physical properties.¹ Photochromic materials of fullerenes,² porphyrins,³ spiroxazines⁴ and stilbene⁵ derivatives belong to the first mentioned category. Classes of compounds with a broad range of potential applications in the second category include fulgides,⁶ diarylethenes⁷ and azo compounds.⁸ With respect to this, interest has also been focused on molecular switches for data storage on the molecular level⁹ to create diodes¹⁰ or other data storage systems.¹¹ Other potential applications result from the combination of photochromic molecules and biological materials.

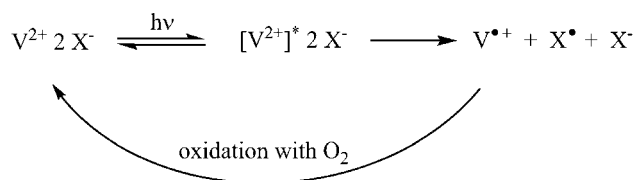
As examples, photobiological switches can release biologically active substances, such as enzymes¹² or biological messengers,¹³ on irradiation.¹⁴ Biomaterials as coatings, which can be reversibly switched on and off, possess potential as biocomputers¹⁵ or biosensors.¹⁶ They translate biochemical processes into electric signals.

Mechanistically, either pericyclic reactions (spiropyranes,¹⁷ spirooxazines,¹⁸ chromenes,¹⁹ fulgides,²⁰ diarylethenes²¹), *cis/trans*-isomerisations (azo compounds,²² anils²³), or electron transfer reactions (viologens) cause photochromism. Photocatalytic reversible electron transfer reactions of viologens,²⁴ including punicin derivatives,²⁵ have also been developed.

Three types of viologen partial structures in materials can be distinguished: viologens in the polymer chain, in the side chain, or in polymer blends. Polyviologens have been known since 1971,²⁶ and viologen-containing films were developed shortly after.²⁷ Some efforts have been devoted to photochromic

materials involving viologen-derived compounds.²⁸ Thus, bis-pyridinium salts are known to be photochromic in aprotic resin matrices. An electron transfer from the anion X^- to the viologen *via* an excited state $[V^{2+}]^*$ was proposed. This transfer results in radical cations $V^{•+}$ which are intensely blue in color (Scheme 1).²⁸

The hitherto studied parameters influencing the photo-responsive properties of viologen derivatives are the polarity of the matrix, the nucleophilicity of the anion in the matrix, and the redox potential of the cation.²⁸ Thus, photochromic behaviour in salts is explained by electron transfer from the anion to the cation, as exemplified by **I** in Fig. 1. An alternative procedure described in the literature is the electron transfer from a sensitizer (S) to the cation (**II**).^{24,25} Electron transfers from the anionic part of mesomeric betaines ("inner salts") into the cationic part (**III**) are scarcely described in the literature, although they play an important role in negatively solvatochromic dyes, such as Reichardt's betaine, to determine solvent polarities.³⁴ This aroused our interest in studying in detail the photoresponsive properties of materials which possess mesomeric betaine partial structures.



Scheme 1

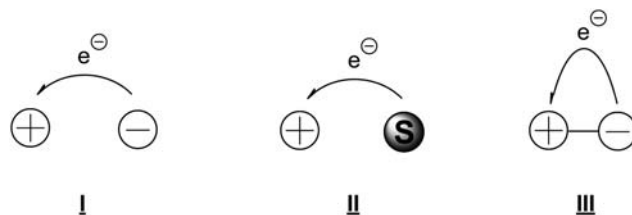


Fig. 1

^aClausthal University of Technology, Institute of Organic Chemistry, Leibnizstrasse 6, D-38678 Clausthal-Zellerfeld, Germany. E-mail: schmidt@ioc.tu-clausthal.de; Fax: +49-(0)5323-722858; Tel: +49-(0)5323-723861

^bClausthal University of Technology, Institute of Physical Chemistry, Arnold-Sommerfeld-Strasse 4, D-38678 Clausthal-Zellerfeld, Germany

^cETH Zürich, Laboratory of Physical Chemistry, HCI F 231, Wolfgang-Pauli-Strasse 10, CH-8093 Zürich, Switzerland

Therefore, we prepared and characterized 4,4'-bipyridine- and 2,4'-bipyridine-functionalized Merrifield resins, *i.e.* polystyrene resins based on a copolymer of styrene and chloromethylstyrene. These resins possess CH-acidic groups which result in the formation of ylides (a subclass of mesomeric betaines) on deprotonation. We present spectroscopic evidence that ylide partial structures cause photochromism, so that our results supplement the knowledge about materials possessing viologen substructures. Furthermore, these materials can be applied in photocatalytic reversible electron transfer reactions. We present our results on syntheses, characterizations, and modes of action, including EPR and HYSCORE measurements as well as the results of DFT calculations.

Experimental

Materials

Merrifield resin crosslinked with 2% DVB, 200–400 mesh was purchased from Fluka. All other chemicals were used without further purification.

Instrumentation

The ^1H and ^{13}C NMR spectra were recorded on Bruker Avance 400 and Avance DPX-200 spectrometers. Chemical shifts δ are reported in ppm. The internal standard was tetramethylsilane for measurements in CDCl_3 and DMSO-d_6 , respectively, and the solvent resonance frequency for measurements in methanol ($\delta = 3.31$ ppm) and water ($\delta = 4.72$ ppm), respectively. Coupling constants J are presented in Hertz (Hz). Multiplicities are described by using the following abbreviations: s = singlet, d = doublet, m = multiplet, b = broad. FT-IR spectra were obtained on a Bruker Vektor 22 in the range of 400–4000 cm^{-1} (2.5% pellets in KBr). The UV-Vis spectra of the model compound **3c** were recorded in methanol with a Hewlett-Packard UV-Vis Diode Array spectrophotometer 8452 A with 10 mm QS-110 tubes (Hellma). UV-Vis spectra of Merrifield resin **6a** were measured on a Jasco V550-spectrometer in the range of 650–300 nm with a spectral resolution of 1 nm. The EI mass spectra were measured with a Hewlett Packard HP 5989, and the ESI mass spectra were measured with an Agilent Series 1100. High resolution electrospray ionization mass spectrometry was performed at the Institute of Organic Chemistry of the University of Hannover (Germany). A TQ-150 medium pressure 150 W mercury lamp (UV-Consulting Peschl, Mainz, Germany) in a pyrex photoreactor was used for the irradiation experiments. Melting points are uncorrected and were determined in an apparatus according to Dr Tottoli (Büchi). Confocal microscopy was performed on a Leica TCS SP2 confocal laser scanning microscope using a water immersion objective (63 \times , NA = 1.2). DFT calculation and simulation of HYSCORE intensities: The spectroscopic parameters of different types of viologen ion-radicals were computed in two steps with the ORCA software.²⁹ First, the geometry optimization was performed (Calculation level – Medium Opt; method – unrestricted Kohn–Sham; functional – BP86; basis set – SV(d)). In the second step, the hyperfine and electric quadrupole tensors were computed (method – unrestricted Kohn–Sham; functional – PBE0; basis set – EPR II). The computed spectroscopic parameters were then used to

simulate the HYSCORE spectra for different viologen ion radicals. The simulations of the nitrogen HYSCORE spectra were performed with the use of a home-written simulation program.³⁰ For the mono-pyridine-based radicals, only one nitrogen nucleus was included in the HYSCORE simulation. For the bipyridine-based radicals, both nitrogen nuclei were included in the simulation and the HYSCORE intensities were computed in accordance with the product rule. The hydrogen nuclei were not included into the simulations. EPR spectroscopy was performed as follows: The continuous wave (CW) EPR spectra were measured with a Miniscope MS200 spectrometer (Magnetech, Germany, mw frequency 9.44 GHz) equipped with a rectangular cavity TE₁₀₂ resonator. The X-band pulse EPR measurements were performed with Bruker E680 X spectrometer. The MD4 dielectric resonator from Bruker BioSpin (mw frequency 9.78 GHz) was used for pulse measurements. All of the pulse measurements were done at 80 K; the sample temperature was stabilized with a He-flow cryostat (CF 935, Oxford Instruments). The HYSCORE experiments were performed with a 24 ns π -pulse and 12 ns $\pi/2$ -pulses. Spectra with two delay times – 112 and 256 ns were measured for both **6a** and **3c**. In addition, the spectra with delay times of 164 and 288 ns were checked for the resin **6a** in order to prove that no additional peaks appear in the HYSCORE pattern. Due to the small widths of the EPR signals of studied species no orientation selection is expected in the measured HYSCORE spectra. EPR sample preparation details are as follows: For light irradiation, a 200 W short arc mercury lamp was used (OmniCure 2000 light source, EXFO Photonic Solutions Inc.). The EPR spectra under light irradiation were measured at room temperature. The oxygen-free NaOH solution in MeOH–EtOH 9 : 1 mixture, as well as the MeOH–EtOH 9 : 1 mixture without NaOH, were prepared by several freeze/pump/thaw cycles. For the monomer **3c**, a given amount of solid powder was dissolved in the oxygen-free NaOH solution in MeOH–EtOH mixture under nitrogen flow. For the resin **6a**, EPR samples were prepared as follows: the resin powder was put into the MeOH–EtOH oxygen-free mixture, stirred and simultaneously titrated with a 100 μM NaOH solution until a slightly noticeable change of the color of resin was visually observed. This procedure allowed the creation of a sufficient number of spatially separated paramagnetic species with relatively weak magnetic dipolar interactions between them. Immediately after preparation, the samples were frozen in liquid nitrogen and were kept frozen in order to prevent diffusion of oxygen into the sample.

N-Phenylmethyl-4,4'-bipyridinium bromide **3a**

A solution of 2.00 g (13 mmol) of 4,4'-bipyridine and 1.20 mL (10 mmol) of benzyl bromide in 100 mL of acetone was heated at reflux temperature for 1 h. The solution was then concentrated to approximately 10 mL and the precipitated solid was filtered off and washed with ether. Yield: 1.59 g (49%) of a slightly greenish solid, mp (dec). 226 °C. δ_{H} (200 MHz; D_2O): 8.93 (d, $J = 6.9$ Hz, 2H), 8.66 (d, $J = 6.1$ Hz, 2H), 8.30 (d, $J = 6.9$ Hz, 2H), 7.79 (d, $J = 6.1$ Hz, 2H), 7.44 (s, 5H), 5.78 (s, 2H). δ_{C} (50 MHz; D_2O): 153.8, 149.9, 144.7, 142.1, 132.5, 129.9, 129.6, 129.1, 126.0, 122.3, 64.2. $\nu_{\text{max}}/\text{cm}^{-1}$: 3423, 3009, 1637, 1547, 1494, 1414, 1225, 1157,

835, 725, 467. C₁₇H₁₅BrN₂ requires: C, 62.40; H, 4.62; N, 8.56. Found: C, 62.25; H, 4.29; N, 8.55.

N'-Phenylmethyl-2,4'-bipyridinium bromide **3b**

A sample of 265 mg (1.7 mmol) of 2,4'-bipyridine was dissolved in toluene and treated with 0.50 mL (4.3 mmol) of benzyl bromide. The mixture was then heated at reflux temperature for 6 h, during which time a solid precipitated, which was filtered off and washed with ether. Yield: 576 mg (100%) of a gray solid, mp 93 °C. δ_{H} (200 MHz; D₂O): 8.90 (d, $J = 7.0$ Hz, 2H), 8.63 (m, 1H), 8.38 (d, $J = 7.0$ Hz, 2H), 8.01 (m, 2H), 7.50 (m, 1H), 7.43 (s, 5H), 5.74 (s, 2H). δ_{C} (50 MHz; D₂O): 153.2, 149.5, 149.3, 144.6, 139.6, 132.6, 130.0, 129.6, 129.1, 126.9, 125.2, 124.2, 64.1. $\nu_{\text{max}}/\text{cm}^{-1}$: 3406, 3003, 1637, 1558, 1513, 1458, 1343, 1160, 1100, 991, 870, 826, 786, 729, 698, 628, 574, 477. HR-ESIMS: 247.1198 (100) [M⁺].

N,N'-Bis-(phenylmethyl)-4,4'-bipyridinium dibromide **3c**

A sample of 750 mg (4.8 mmol) of 4,4'-bipyridine was dissolved in 20 mL acetonitrile. After addition of 1.14 mL (9.6 mmol) benzylbromide, the mixture was heated at reflux temperature for 5 h. The resulting precipitate was filtered off and washed with dichloromethane. Yield: 2.22 g (93%) of a light yellow solid, mp. 260 °C (decomposition). δ_{H} (400 MHz, D₂O): 9.07 (d, $J = 6.6$ Hz, 4H), 8.44 (d, $J = 6.6$ Hz, 4H), 7.44 (s, 10H), 5.84 (s, 4H). δ_{C} (100 MHz, D₂O): 150.2, 145.4, 132.1, 130.1, 129.6, 129.3, 127.1, 64.7. The NMR data are in accordance with those reported in the literature.³¹

N-Phenylmethyl-*N'*-methyl-4,4'-bipyridinium bromide iodide **3d**

A sample of 208 mg (0.6 mmol) of *N*-phenylmethyl-4,4'-bipyridinium bromide **4a** was dissolved in acetonitrile at reflux temperature. After the addition of 0.2 mL (3 mmol) of methyl iodide, the mixture was heated for 4 h, during which time a precipitate formed. After cooling, the solid was filtered off and washed with ether to yield 250 mg (83%) of a red solid, mp. 233 °C. δ_{H} (200 MHz, D₂O): 9.11 (d, $J = 7.0$ Hz, 2H), 9.00 (d, $J = 6.8$ Hz, 2H), 8.51 (m, 4H), 7.48 (s, 4H), 5.88 (s, 2H), 4.44 (s, 3H). δ_{C} (50 MHz, D₂O): 150.3, 149.6, 146.3, 145.5, 132.1, 130.1, 129.6, 129.3, 127.1, 126.7, 64.8, 48.4. $\nu_{\text{max}}/\text{cm}^{-1}$ 3449, 3001, 1636, 1556, 1495, 1450, 1358, 1272, 1229, 1184, 797, 730, 470. HR-ESIMS: 262.1826 (13) [M⁺].

[*N*-Methyl-(4,4'-bipyridinium)]-polystyrene polychloride **6a**

A suspension of 3.0 g of Merrifield resin in 250 mL of dioxane was stirred for 1 h at rt. Then, 4.3 g (27.6 mmol) of 4,4'-bipyridine was added, and the resulting mixture was heated at reflux temperature for 48 h. The precipitate was collected by filtration and washed with dioxane. Yield: 5.1 g. $\nu_{\text{max}}/\text{cm}^{-1}$: 3422, 2922, 1635, 1490, 1444, 1154, 812, 701. CHN analysis: Found: C, 67.03; H, 6.37; N, 4.83.

[*N'*-Methyl-(2,4'-bipyridinium)]-polystyrene polychloride **6b**

A suspension of 250 mg of Merrifield resin in 25 mL of dioxane was stirred for 1 h at rt. Then, 215 mg (1.4 mmol) of 2,4'-

bipyridine was added. After heating at reflux temperature for 48 h, the solid was collected by filtration and washed with dioxane. Yield: 420 mg of a slightly brownish solid. $\nu_{\text{max}}/\text{cm}^{-1}$: 3424, 2921, 1634, 1509, 1449, 1424, 1153, 1116, 989, 870, 811, 783, 697, 534. CHN analysis: Found: C, 69.73; H, 5.92; N, 5.49.

Anion exchange reaction of **6a** with sodium tetrafluoroborate

A suspension of 511 mg [*N*-methyl-(4,4'-bipyridinium)]-polystyrene polychloride **6a** and 1.1 g sodium tetrafluoroborate in 6 mL of distilled water was stirred for 48 h at room temperature. The resulted solid was filtered off and washed with distilled water. Yield: 499 mg of a yellow solid. Found: C, 71.25, H, 6.41, N, 5.50.

Dimethyl-3-phenyl-7-(pyridin-4-yl)-indolizine-1,2-dicarboxylate³² **9a**

A two-phase system of 189 mg (0.6 mmol) of *N*-phenylmethyl-4,4'-bipyridinium bromide, 12 mL of 50% aqueous potassium carbonate and 6 mL of dichloromethane was treated with 99 mg (0.7 mmol) of dimethyl acetylenedicarboxylate. The mixture was stirred for 2.5 h at rt and then extracted three times with 10 mL of dichloromethane, respectively. The organic layer was dried over magnesium sulfate and evaporated to dryness *in vacuo*. The residue was chromatographed (silica gel; ethyl acetate-*n*-hexane = 4 : 1. Yield: 77 mg (34%) of an orange-colored solid, mp. 132 °C. δ_{H} (200 MHz, CDCl₃): 8.67 (dd, $J = 4.6$ Hz, $J = 1.7$ Hz, 2H), 8.57 (m, 1H), 8.13 (dd, $J = 7.4$ Hz, $J = 0.9$ Hz, 1H), 7.58 (dd, $J = 4.6$ Hz, $J = 1.7$ Hz, 2H), 7.51 (m, 5H), 7.01 (dd, $J = 7.4$ Hz, $J = 2.0$ Hz, 1H), 3.92 (s, 3H), 3.81 (s, 3H). δ_{C} (50 MHz, CDCl₃): 166.5, 164.1 150.5, 145.6, 134.9, 132.9, 129.9, 129.3, 129.2, 128.5, 125.6, 124.1, 122.9, 120.9, 118.2, 112.1, 103.6, 52.6, 51.5. $\nu_{\text{max}}/\text{cm}^{-1}$: 2924, 1732, 1696, 1592, 1516, 1448, 1209, 1062, 782, 702. m/z (%): 386 (100) [M], 328 (7), 268 (26), 191 (13). HR-ESIMS: 387.1659 (100) [M⁺].

Methyl-3-phenyl-7-(pyridin-4-yl)-indolizine-1-carboxylate³² **9b**

A two-phase system consisting of 189 mg (0.6 mmol) of *N*-phenylmethyl-4,4'-bipyridinium bromide, 12 mL of 50% aqueous potassium carbonate and 9 mL of dichloromethane was treated with 0.06 mL (0.7 mmol) of methylpropiolate. The mixture was then stirred at rt for 2.5 h and finally extracted three times with 10 mL of dichloromethane, respectively. The organic layer was dried over magnesium sulfate and evaporated to dryness *in vacuo*. The residue was then chromatographed (silica gel, ethyl acetate-*n*-hexane = 4 : 1). Yield: 38 mg (20%) of an orange-colored solid, mp. 130 °C. δ_{H} (200 MHz, CDCl₃): 8.68 (d, $J = 6.1$ Hz, 2H), 8.62 (m, 1H), 8.36 (dd, $J = 7.4$ Hz, $J = 0.9$ Hz, 1H), 7.59 (d, $J = 6.1$ Hz, 2H), 7.51 (m, 5H), 7.33 (s, 1H), 6.99 (dd, $J = 7.4$ Hz, $J = 2.0$ Hz, 1H), 3.93 (s, 3H); δ_{C} (50 MHz, CDCl₃): 165.1, 150.4 145.8, 136.0, 131.4, 130.7, 129.2, 128.5, 128.3, 127.1, 123.8, 120.8, 117.9, 117.0, 111.1, 105.8, 51.1. $\nu_{\text{max}}/\text{cm}^{-1}$: 2948, 1691, 1598, 1517, 1440, 1410, 1211, 1050, 765, 707. m/z (%): 327 (100) [M-1], 270 (13), 268 (26), 192 (5), 79 (61). HR-ESIMS: 329.1273 (100) [M⁺].

Dimethyl-3-phenyl-7-(pyridin-2-yl)-indolizine-1,2-dicarboxylate³² **9c**.

A two-phase system consisting of 189 mg (0.58 mmol) of *N'*-phenylmethyl-2,4'-bipyridinium bromide, 12 mL of 50% aqueous potassium carbonate and 6 mL of dichloromethane was treated with 99 mg (0.7 mmol) of dimethyl acetylenedicarboxylate. The mixture was then stirred for 2.5 h at rt and finally extracted with four portions of 20 mL of dichloromethane. The organic layer was dried over magnesium sulfate and evaporated to dryness *in vacuo*. The residue was then chromatographed (silica gel; *n*-hexane–ethyl acetate = 2 : 1). Yield: 68 mg (30%) of a yellow solid, mp. 134 °C. δ_{H} (200 MHz, CDCl₃): 8.71 (m, 1H), 8.60 (m, 1H), 8.04 (dd, $J = 7.4$ Hz, $J = 1.0$ Hz, 1H), 7.81 (d, $J = 7.0$ Hz, 1H), 7.69 (m, 1H), 7.51–7.39 (m, 6H), 7.17 (m, 1H), 3.85 (s, 3H), 3.73 (s, 3H). δ_{C} (50 MHz, CDCl₃): 166.7, 164.2, 154.7, 149.7, 136.9, 135.1, 134.6, 129.8, 129.1, 128.7, 125.4, 123.8, 122.9, 122.7, 120.5, 117.6, 112.4, 103.3, 52.5, 51.4. $\nu_{\text{max}}/\text{cm}^{-1}$: 2924, 1723, 1681, 1515, 1448, 1382, 1213, 776, 695. m/z (%): 386 (100) [M], 328 (10), 268 (13), 191 (11), 78 (21). HR-ESIMS: 387.1567 (100) [M⁺].

N-(1-Methyl-1-phenylethyl)-4,4'-bipyridinium tetrafluoroborate **11**

A sample of 250 mg (1.6 mmol) of 2-chloro-2-phenyl-propane **10**³³ was dissolved in 5 mL abs. nitromethane. Then, 750 mg (4.8 mmol) 4,4'-bipyridine and 310 mg (1.6 mmol) silver tetrafluoroborate were added. The resulting solid was filtered off and the filtrate was concentrated to approximately 5 mL. After addition of diethylether, the resulting solid was filtered off and washed with dichloromethane to obtain 102 mg of 1 : 1 mixture of the desired product and the corresponding bipyridinium salt. δ_{H} (200 MHz, DMSO): 9.22 (d, $J = 7.1$ Hz, 2H), 8.87 (d, $J = 6.0$ Hz, 2H), 8.57 (d, $J = 7.1$ Hz, 2H), 8.06 (d, $J = 6.0$ Hz, 2H), 7.44 (m, 5H), 2.20 (s, 6H). HR-ESIMS: 275,1539 (27) [M⁺].

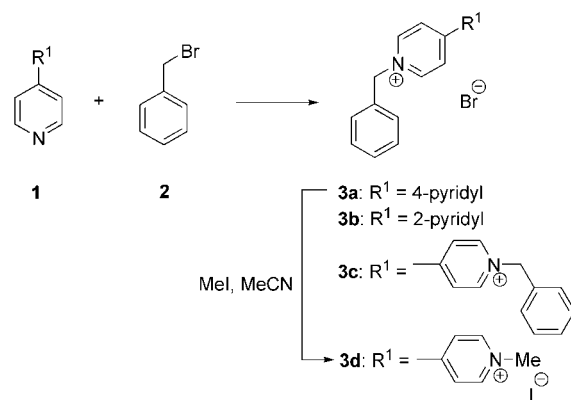
Results and discussion

1. Syntheses and characterizations of model compounds and modified Merrifield resins

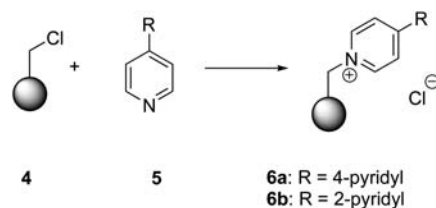
Reaction of pyridines **1** with benzyl halides **2** by standard procedures, in acetone according to modified literature procedures, resulted in the formation of the pyridinium salts **3a,b** (Scheme 2). Reaction of 4,4'-bipyridine with two equivalents of benzyl bromide **2** yielded the bipyridinium salt **3c**. Methylation of **3a** with methyl iodide in acetonitrile gave the bipyridinium salt **3d**.

The Merrifield resin-bound pyridinium salts **6a,b** were prepared starting from commercially available Merrifield resin **4** with the corresponding pyridines **5** in dioxane. The resins **6a,b** precipitated and were collected by filtration (Scheme 3).

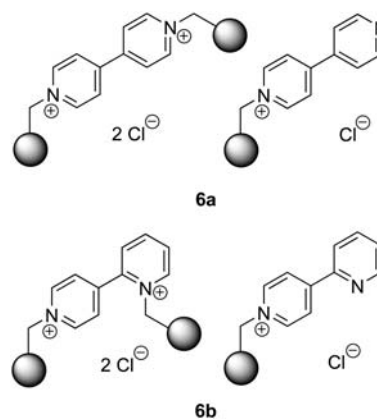
Whereas 4,4'-bipyridine is able to form links between two resin backbones under formation of viologen partial structures (*cf.* **6a**), cross-links are less probable starting from 2,4'-bipyridine, as the latter mentioned compound did not react with benzyl halides at the 2-, but exclusively at the 4'-position (*cf.* **6b**) (Scheme 4). The elemental analyses reveal that approximately 2/3 of the chlorobenzyl groups are substituted. A lower degree of substitution can be adjusted stoichiometrically.



Scheme 2



Scheme 3



Scheme 4

In order to obtain a different anion, an aqueous suspension of **6a** was treated with sodium tetrafluoroborate, filtered off, and washed with water. The anion exchange was proved by elemental analysis.

2. Photochromic properties

The resins **6a,b** as chlorides and **6a** as tetrafluoroborate display strong photochromism in the solid state on exposure to sunlight or UV light. Thus, they change their color from yellow and slightly brownish, respectively, to dark blue and reddish brown. Exposure of the resin to air in the dark reconstitutes the original color within a few minutes.

UV spectra of the polymer **6a** were measured on fixing a polystyrene film containing 10% of the Merrifield resin between two quartz plates. For the irradiation experiments, the sample

holder had to be taken out of the spectrometer and, therefore, the spectra had to be corrected to account for differences in the sample holder position. The absorption spectra were shifted and stretched to give a maximal overlap in the range from 300 to 330 nm. In this range, absorption from the dye was now observed. The baseline underlying the spectra shows a λ^{-4} -dependence, as expected for the wavelength-dependent turbidity of the strongly scattering Merrifield particles. On irradiation, an absorption band at 608 nm develops, while the shoulder at 350–425 nm disappears (Fig. 2). After 8 min in the dark, the intensity of the band at 608 nm decreases (Fig. 3 and 4). To visualize the bleaching process, UV-Vis spectra of the irradiated Merrifield particles **6a** were measured after specific periods of time during the exposure to air. This is connected with a stepwise decrease of the characteristic absorption band at 608 nm (Fig. 3). UV-Vis spectra of the monomer **3c** ($c = 0.4 \text{ mmol L}^{-1}$) show two bands at 208 and 262 nm at pH 7, whereas addition of aqueous 0.1 M NaOH gives a dark blue solution with absorption maxima at 400 and 606 nm. On addition of HCl, this process is reversible.

To localize the active photochromic centres on the resins, compounds **6a** and **6b** were irradiated near their excitation

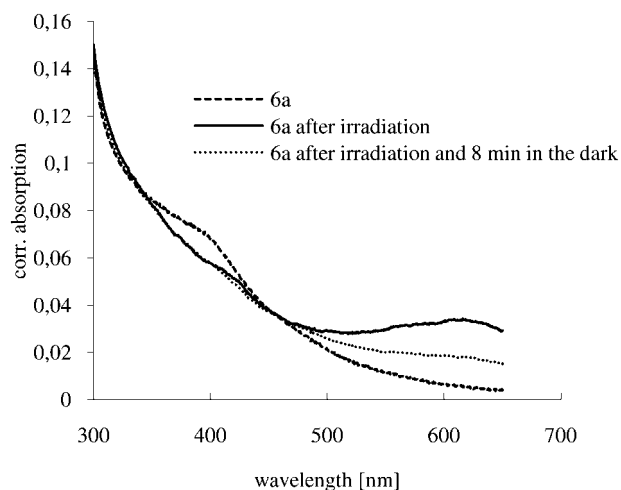


Fig. 2 Solid state UV spectra of resin **6a** on irradiation in the range of 300–650 nm.

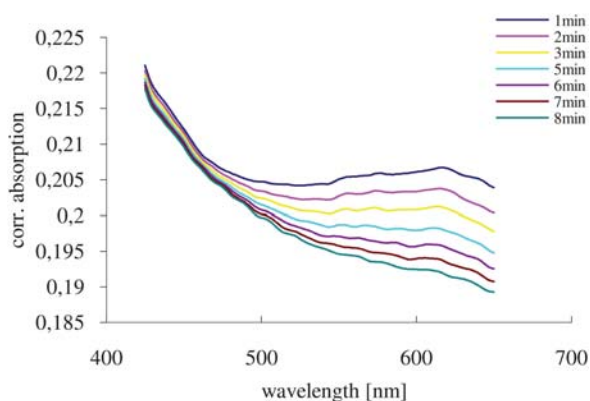


Fig. 3 Solid state UV spectra of resin **6a** on irradiation in the range of 400–650 nm. The maximum decreases with time after irradiation.



Fig. 4 Substituted Merrifield resin **6a** before and after irradiation with UV light.

wavelength at 468 and 406 nm, respectively, under the confocal laser scanning microscope in the solid state. By detection of the emission intensity at 545 nm (**6a**) and 498 nm (**6b**), the process of the photochromism can be pursued. Fig. 5 shows spherical particles of resin **6a** with diameters in the range of 95 μm , on which the color centres, as the emitted radiation indicates, were mainly situated on the surface. Irradiation causes a change in color from yellow to blue during the photochromic process. This is connected with a shift of the excitation wavelength so that the intensity decreases (upper right image). After ten minutes in the dark an increasing value of the emitted light can be observed, especially in the centre of the particles, which is a result of

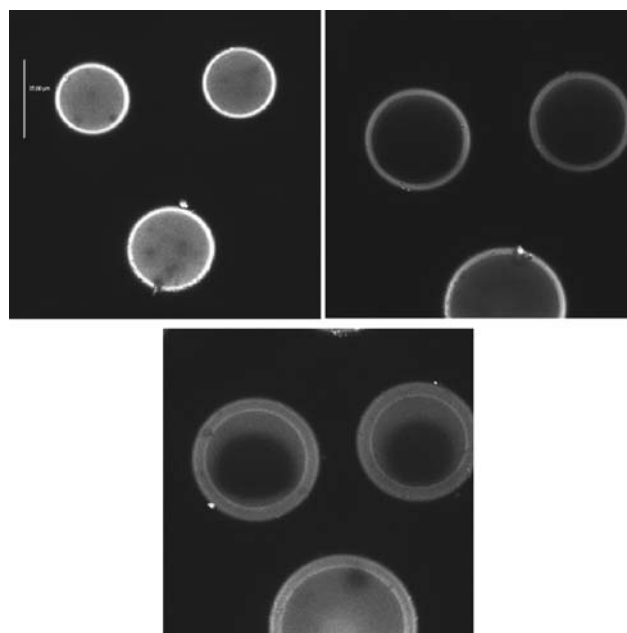


Fig. 5 Images of Merrifield resin **6a** under the confocal laser scanning microscope before (upper left), after (upper right) and ten minutes after irradiation (bottom). The apparent difference in the particle diameters in the three images is a result of the fact that the location of the focal-plane of the microscope is sectioning the particles at different locations.

reconstitution of the original yellow color by contact of oxygen with the resin (bottom image).

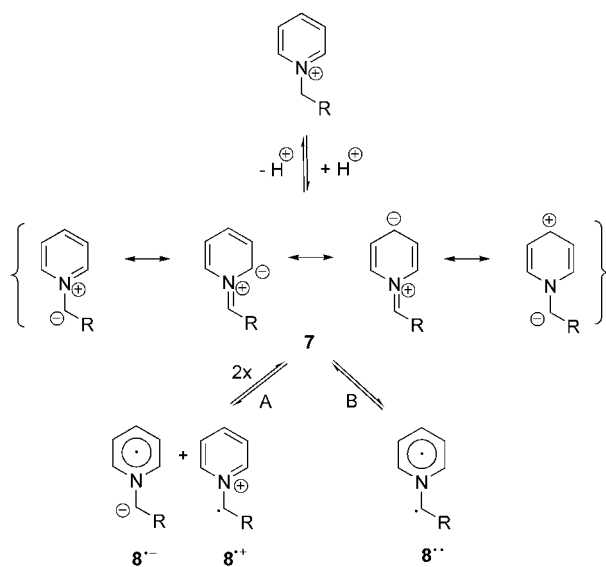
Examination of compound **6b** supplies similar results. The photochromic centres were also mainly localized on the surface of the particles, and the bleaching process can be observed during irradiation of the resin by light near its excitation wavelength.

3. Mode of action

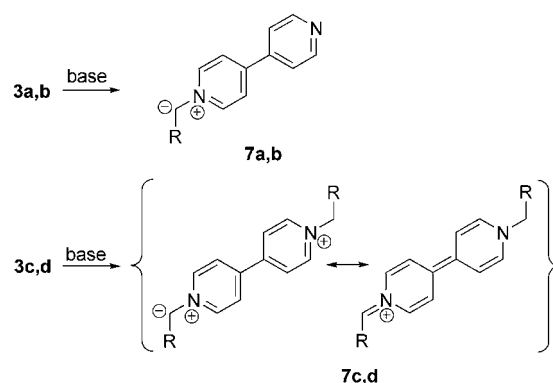
Due to the C–H acidity of the methylene bridge between the phenyl ring of the Merrifield backbone and the pyridinium rings, ylides **8** are formed by deprotonation (Scheme 5). Ylides belong to the class of conjugated heterocyclic mesomeric betaines and can be represented by several canonical formulae, as shown. *A priori*, disproportionations of ylide **8** into the anion radical $8^{\cdot-}$ (π -radical) and the radical cation $8^{\cdot+}$ (α -radical, pathway A), or intramolecular electron transfers to the diradical $8^{\cdot\cdot}$, can be envisaged (pathway B). In these inner salts, the anionic partial structure played the role of the electron donating species.

As a matter of fact, on addition of base to the modified Merrifield resins **6a,b**, as well as to the model compounds **3a–d**, intense changes of color are observable. On addition of acid, the original colors are reconstituted. We examined these ylides spectroscopically, performed model reactions, and measured and calculated EPR and HYSCORE spectra to elucidate a possible relationship between ylide formation, photochromism, and indicator properties of *N*-benzylpyridinium salts as model compounds and as partial structures of Merrifield resins.

On treatment with base, the model compounds **3a–d** form 1,2-ylides **7a–d**. The ylides **7c,d** are stabilized by the second positive charge which allows the formulation of a neutral canonical formula (Scheme 6). As a consequence, they are more stable than those formed from **3a,b**, as evidenced by spectroscopic methods. In electrospray ionization mass spectrometry, compound **3a** sprayed from methanol in the presence of potassium carbonate gives the peaks of the ylide **7a** at $m/z = 285.1$ [ylide + K]⁺ at 0 V fragmentor voltage. Likewise, the dication of **3c** gives a peak at



Scheme 5



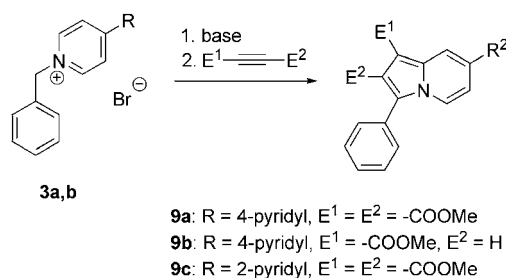
Scheme 6

$m/z = 169.1$ [M/2]⁺ and the ylide **7c** at $m/z = 337.1$ [M – H]⁺; the solution is intensely blue in color on addition of the base. As expected, **3a** possesses two H/D-exchangeable positions: a solution of **3a** in D₂O exchanges the α -position of the pyridinium ring and the benzylic protons as observable by ¹H NMR spectroscopy. Similar results were obtained with **3b** and **3d**.

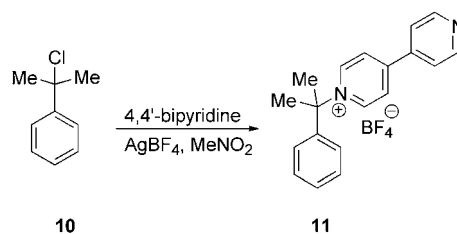
In preparative scale, the ylides of **3a,b** can be trapped with activated acetylenes by 1,3-dipolar cycloadditions as **9a–c** (Scheme 7).

A blind probe was performed as follows: to generate a pyridinium salt without an exocyclic CH-acidic position attached to nitrogen, we reacted 2-chloro-2-phenylpropane **10** according to a procedure by Katritzky³⁵ with 4,4'-bipyridine in the presence of a silver tetrafluoroborate, and obtained **11** (Scheme 8). As expected, no color change is observable on addition of base.

In order to get insight into the structure of the colored species, a series of EPR measurements was performed. Both the light irradiation and the treatment with NaOH lead to the same color change of **6a** and produced very similar EPR signals at $g \approx 2.006$



Scheme 7



Scheme 8

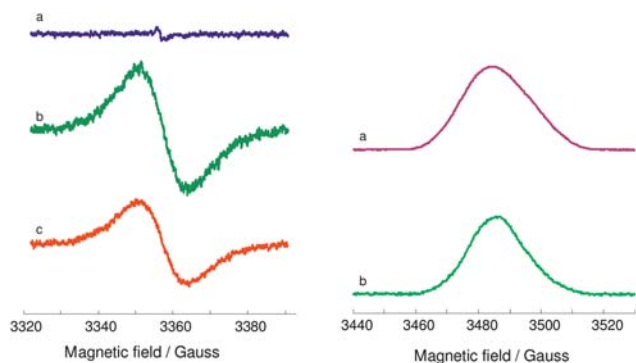


Fig. 6 (Left) CW EPR spectra of the compound **6a** under light irradiation: (a) background spectrum with weak signal from paramagnetic impurities, (b) the spectrum under irradiation, (c) the spectrum measured approx. 10 min after the irradiation was switched off; (right) the Hahn echo detected EPR spectra of the resin **6a** (a) and monomer **3c** (b) in NaOH/EtOH–MeOH. Spectra are recorded at 80 K with interpulse delay time of 112 ns.

(Fig. 6, left). In the irradiated sample the local concentration of the paramagnetic centers appeared to be very high. This resulted in short relaxation times for the paramagnetic species, which did not allow for pulse EPR experiments. In contrast to the light irradiation experiment, the titration with NaOH provided a more controlled way of creating ion-radicals. The formed paramagnetic species gave rise to a single asymmetric EPR signal with a slight g -anisotropy ($\Delta g \approx 0.004$, Fig. 6, right). Considering the rather small g -anisotropy of the signal, the formation of triplet species, such as $\mathbf{8}^{*}$ in Scheme 5, seems to be highly improbable. Therefore, the paramagnetic species rather appear *via* creation of cation/anion radical pairs. For the monomer solution of **3c**, the recombination of ion-radicals with the formation of diamagnetic species is known to happen at low temperatures.³⁶ Freezing by immersion of the sample tube into liquid nitrogen was not fast

enough to avoid this process. Effectively, a maximum concentration of ion-radicals in the order of 100–200 μM was achieved in the frozen state, which led to significantly worse signal-to-noise ratios in the spectra of monomer samples. The compound **3a** also formed a light blue solution when mixed with NaOH/MeOH–EtOH under oxygen-free conditions, but upon freezing, the color changed immediately to deep rose-red and no paramagnetic species could be detected by EPR. When exposed to air at room temperature, the blue solution of **3a** was also noticeably less stable as compared to **3c**.

The experimental HYSCORE spectra for the compounds **6a** and **3c** are presented in Fig. 7 (only the nitrogen region is shown). One can see considerable similarities in the spectra of the two species. Most regions with significant signal intensity are present for both samples. Nevertheless, local intensity patterns are somewhat different. In order to analyse the experimental data we performed a series of DFT computations of the nitrogen hyperfine and quadrupole tensors for the radical species of the type $\mathbf{8}^{*-}$ (π -radical) and $\mathbf{8}^{*+}$ (α -radical) as well as for similar species formed from compounds **3a** and **3c**. The corresponding spectroscopic parameters are listed in Table 1. The HYSCORE spectra of these species computed with the spectroscopic parameters from DFT calculations are shown in Fig. 8.

Two nitrogen nuclei from the bipyridine fragment are spectroscopically quite different, not only in the case of the α -radical, but surprisingly also for the π -radical species. This indicates that the spin-density is more localized on the side of the molecule where the proton is missing. In turn, the computed hyperfine parameters for the mono-pyridine-based radical species do not much exceed the ones for the stronger coupled nitrogen from bipyridine-based radical species. Nevertheless, in the experiment, the formation of only mono-pyridine-based species can be excluded since they do not feature the second, more weakly, coupled nitrogen nucleus, and therefore cannot be responsible for the signals in the range below approx. 4 MHz. Generally, the

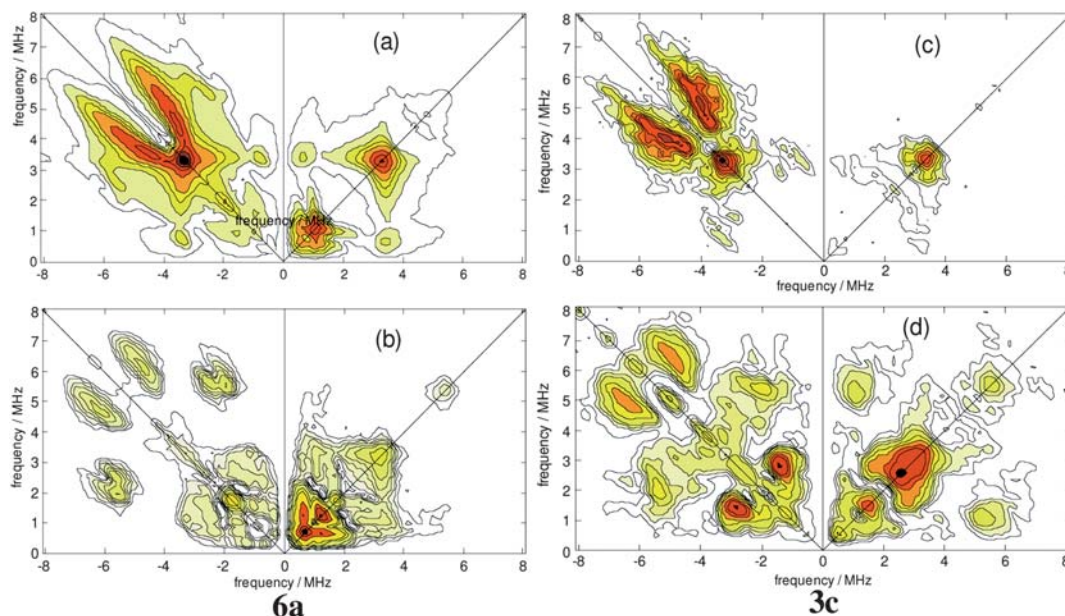


Fig. 7 Experimental HYSCORE spectra for the compounds **6a** and **3c** in the NaOH/MeOH–EtOH solution. (a) **6a**, $\tau = 112$ ns; (b) **6a**, $\tau = 256$ ns; (c) **3c**, $\tau = 112$ ns; (d) **3c**, $\tau = 256$ ns.

Table 1 The DFT computed parameters of the electric quadrupole tensor (e^2qQ , η) and of the hyperfine tensor (A_1 , A_2 , A_3) for some relevant viologen-type radical-ions

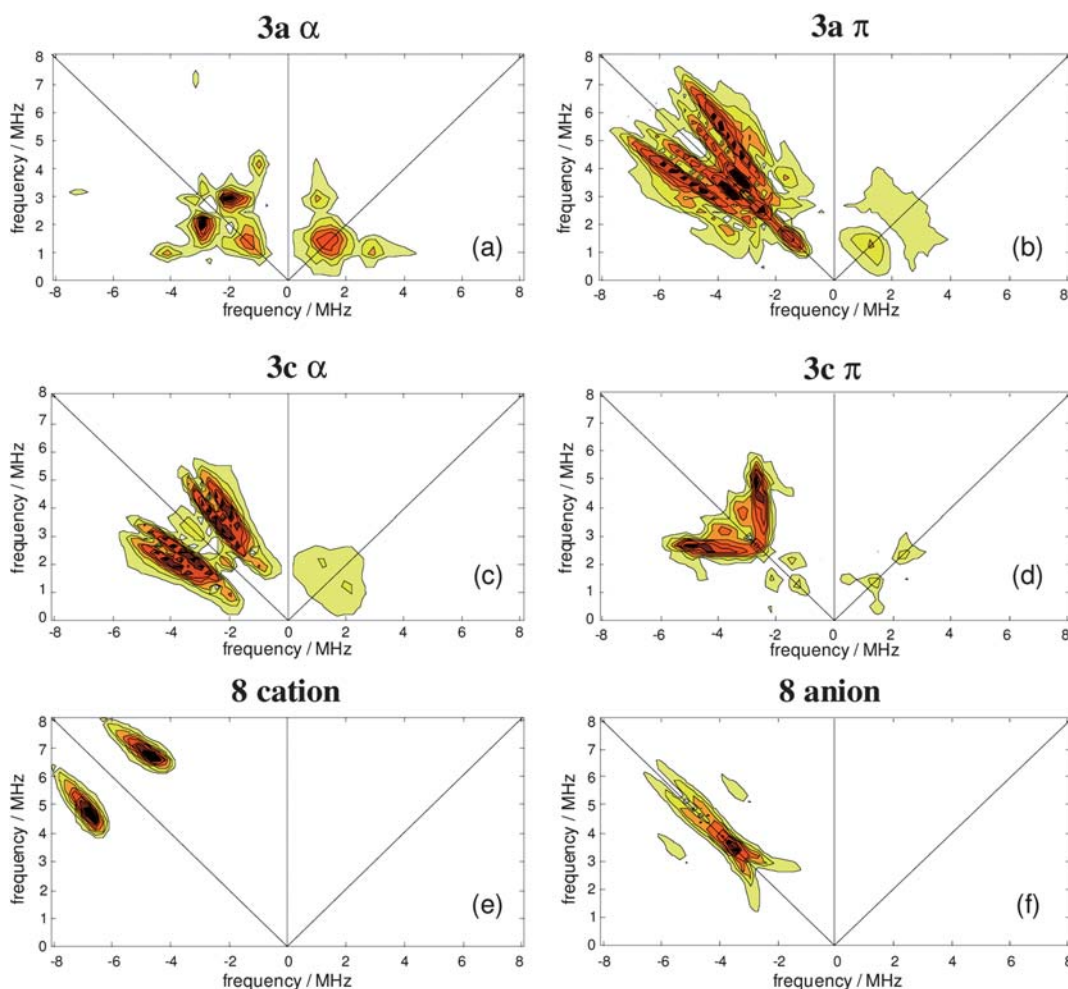
Radical type	Nitrogen atom	e^2qQ/MHz	η	$A_1, A_2, A_3/\text{MHz}$
$8^{+\cdot}$	N1	-1.137	0.070	-10.1804; -10.4090; -21.8989
$8^{-\cdot}$	N1	-3.492	0.099	2.3166; 2.4034; 50.6068
3a α -radical	N1	-1.321	0.061	-9.7820; -10.0623; -21.7443
	N2	-4.978	0.314	-0.1433; -0.2072; 5.3033
3a π -radical	N1	-2.549	0.083	2.2992; 2.4033; 36.0783
	N2	-3.359	0.264	-0.1692; 0.1906; 16.5834
3c α -radical	N1	-1.321	0.080	-8.5635; -8.8139; -17.6344
	N2	-0.974	0.631	0.8669; 1.0439; 9.4956
3c π -radical	N1	-4.303	0.084	-0.1381; -0.2271; 19.2006
	N2	-2.467	0.029	-1.4835; -1.8579; 8.9325

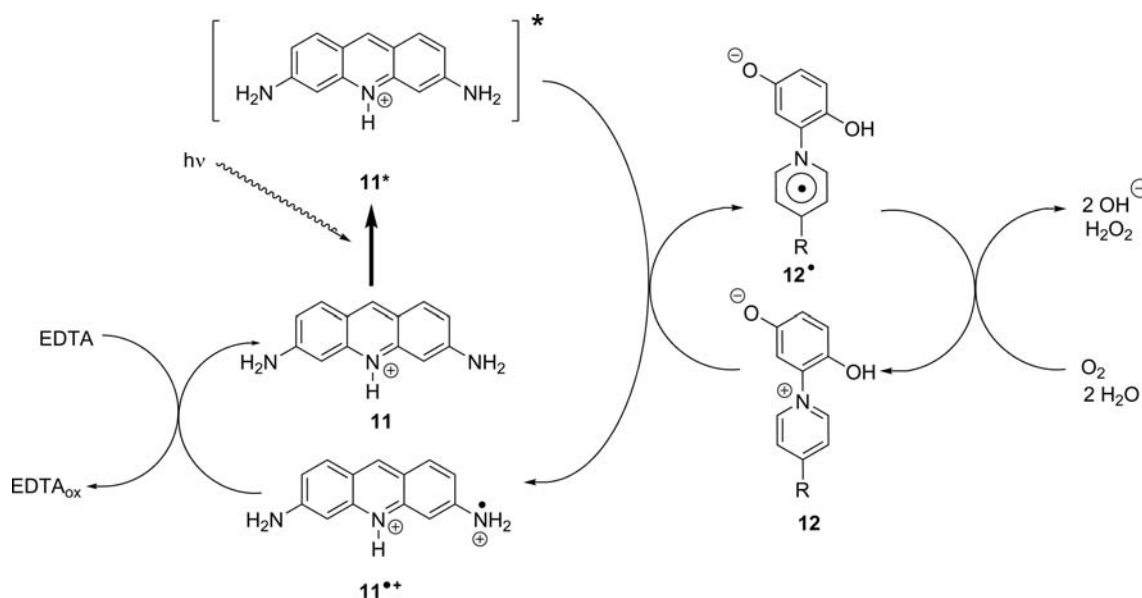
formation of ion-radical species from **3c** fits rather unambiguously to the set of experimental and simulated data. The presence of the paramagnetic centers deriving from **3a** is less probable due to their instability. Still, the spectroscopic parameters of these species are also consistent with the experimental data. If incorporation into the resin matrix can increase their stability, the ion radical species based on **3a** might also be present. In any case,

recombination on freezing would be strongly reduced for all of the bipyridine centers bound to the resin chain.

4. Photocatalytic activities

4,4'-Bipyridinium derivatives can also be used in coupled photocatalytic electron transfers (Scheme 9).²⁵ In this redox cycle,

**Fig. 8** DFT-based simulated HYSCORE spectra for different compounds with $\tau = 112$ ns. (a) cation-radical (α -radical) from **3a**; (b) anion-radical (π -radical) from **3a**; (c) α -radical from **3c**; (d) π -radical from **3c**; (e) α -radical from **7**; (f) π -radical from **7**.



Scheme 9

radicals such as 13^{\bullet} are generated by irradiation in the presence of proflavium 12 as a sensitizer in aqueous solution. The resulting radical species 13^{\bullet} are visually observable by their greenish blue color under an inert atmosphere. The oxidized sensitizer $12^{\bullet+}$ is reduced by ethylenediamine tetraacetate (EDTA), which serves as a sacrificial donor in this redox system.

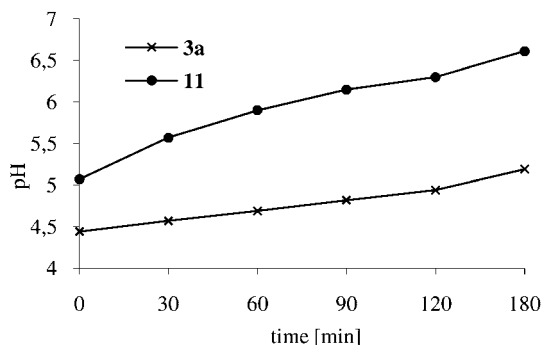


Fig. 9 Photocatalytic electron transfers of the monomers **3a** and **11** with exposure to air as shown in Scheme 9.

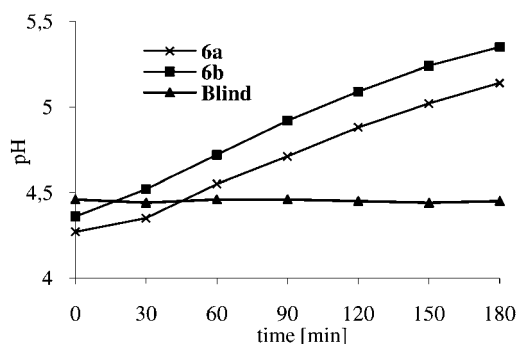


Fig. 10 Photocatalytic electron transfers of the resins **6a,b** with exposure to air as shown in Scheme 9.

Exposure to oxygen (air) regenerates the salt **13** by reoxidation of the radical 13^{\bullet} . This process is accompanied by a change of the color, from greenish blue to light yellow, and an increasing pH value caused by the formation of hydroxide ions on quenching.

We finally measured the change of the pH of compounds **3a**, **6a**, **6b** and **11** in solutions or suspensions with EDTA and proflavium as a sensitizer in water during irradiation with a UV lamp and exposure to air. Both the examined resins and the monomeric model compounds are able to undergo these coupled photocatalytic electron transfers (Fig. 9 and 10). Especially, the activity of **11** in combination with its not observable change in color by addition of base suggests the conclusion that the formation of an *N*-ylide is not required in this redox cycle, but essential for the photochromic properties of this type of compounds in solution at different pH values (Fig. 9).

Conclusions

Spectroscopic evidence by EPR and HYSOCRE techniques prove that mesomeric betaines, present as ylidic partial structures of 4,4'-bipyridine and 2,4'-bipyridine-functionalized Merrifield resins, are additional parameters which cause photochromism of viologen-derived materials. These results are supported by reactions with model compounds which are characterized spectroscopically. Furthermore, we show that these resins can successfully be applied in photocatalytic reversible electron transfer reactions. Thus, our results supplement the knowledge about materials possessing viologen substructures, and can serve as a stimulus for ongoing research and the search for novel applications of viologens and related species.

References

- 1 H. Bouas-Laurent and H. Dürr, *Pure Appl. Chem.*, 2001, **73**, 639.
- 2 P. A. Liddell, G. Kodis, A. L. Moore, T. A. Moore and D. Gust, *J. Am. Chem. Soc.*, 2002, **124**, 7668; P. A. Liddell, G. Kodis, J. Andréasson, L. de la Garza, S. Bandyopadhyay, R. H. Mitchell, T. A. Moore, A. L. Moore and D. Gust, *J. Am. Chem. Soc.*, 2004,

- 126, 4803; S. D. Straight, J. Andréasson, G. Kodis, A. L. Moore, T. A. Moore and D. Gust, *J. Am. Chem. Soc.*, 2005, **127**, 2717.
- 3 Y. Liu, M. Fan, S. Zhang and J. Yao, *J. Phys. Org. Chem.*, 2007, **20**, 884; J. T. Dy, R. Maeda, Y. Nagatsuka, K. Ogawa, K. Kamada, K. Ohta and Y. Kobuke, *Chem. Commun.*, 2007, 5170; T. B. Norsten and N. R. Branda, *J. Am. Chem. Soc.*, 2001, **123**, 1784.
- 4 Y. Hur, M. Lee, S.-H. Jin, Y.-S. Gal, J.-H. Kim, S.-H. Kim and K. Koh, *J. Appl. Polym. Sci.*, 2003, **90**, 3459; S.-H. Kim, C. Yu, C.-J. Shin and M.-S. Choi, *Dyes Pigm.*, 2007, **75**, 250; S. Choi, S. Jin, Y. Gal, J. Kim, S. Kim and K. Koh, *Mol. Cryst. Liq. Cryst.*, 2002, **377**, 229; K. Ock, S. Jin, Y. Gal, J. Kim, S. Kim and K. Koh, *Mol. Cryst. Liq. Cryst.*, 2002, **377**, 233.
- 5 R. Rojanathanes, T. Tuntulani, W. Bhanthumnavin and M. Sukwattanasinitt, *Org. Lett.*, 2005, **7**, 3401; V. Papper and G. I. Likhtenshtein, *J. Photochem. Photobiol., A*, 2001, **140**, 39; A. E. Clark, *J. Phys. Chem. A*, 2006, **110**, 3790; D. Dantsker, *J. Nonlinear Opt. Phys. Mater.*, 1996, **5**, 775.
- 6 Y. Yokoyama, *Chem. Rev.*, 2000, **100**, 1717; M. Seibold, M. Handschuh, H. Port and H. C. Wolf, *J. Lumin.*, 1997, **72–74**, 454; S. Rath, M. Heilig, H. Port and J. Wrachtrup, *Nano Lett.*, 2007, **7**, 3845.
- 7 K. Uchida, A. Tarata, S. Ryo, M. Saito, M. Muratami, Y. Ishibashi, H. Miyasaka and M. Irie, *J. Mater. Chem.*, 2005, **15**, 2128; K. Matsuda and M. Irie, *Polyhedron*, 2005, **24**, 2477; M. Hoshino, F. Ebisawa, T. Yoshida and K. Sukegawa, *J. Photochem. Photobiol., A*, 1997, **105**, 75; H. Tian and S. Yang, *Chem. Soc. Rev.*, 2004, **33**, 85.
- 8 M. Z. Alam, T. Yoshioka, T. Ogata, T. Nonaka and S. Kurihara, *Chem.–Eur. J.*, 2007, **13**, 2641; L. Angiolini, T. Benelli, L. Giorgini, F. Mauriello and E. Salatelli, *Macromol. Chem. Phys.*, 2006, **207**, 1805; I. Conti, F. Marchioni, A. Credi, G. Orlandi, G. Rosini and M. Garavelli, *J. Am. Chem. Soc.*, 2007, **129**, 3198.
- 9 C. C. Corredor, Z.-L. Huang and K. D. Belfield, *Adv. Mater.*, 2006, **18**, 2910; J.-F. Masson, P. A. Liddell, S. Banerji, M. Battaglia, D. Gust and K. S. Booksh, *Langmuir*, 2005, **21**, 7413; W. Yuan, L. Sun, H. Tang, Y. Wen, G. Jiang, W. Huang, L. Liang, Y. Song, H. Tian and D. Zhu, *Adv. Mater.*, 2005, **17**, 156; S.-J. Lim, B.-K. An, S. D. Jung, M.-A. Chung and S. Y. Park, *Angew. Chem.*, 2004, **116**, 6506; S.-J. Lim, B.-K. An, S. D. Jung, M.-A. Chung and S. Y. Park, *Angew. Chem., Int. Ed.*, 2004, **43**, 6346.
- 10 T. Shiono, T. Itoh and S. Nishino, *Jpn. J. Appl. Phys.*, 2005, **44**, 3559; P. Andersson, N. D. Robinson and M. Berggren, *Adv. Mater.*, 2005, **17**, 1798.
- 11 T. Tsujioka, N. Iefuji, A. Jiapaer, M. Irie and S. Nakamura, *Appl. Phys. Lett.*, 2006, **89**, 222102.
- 12 A. D. Turner, S. V. Pizzo, G. Rozakis and N. A. Porter, *J. Am. Chem. Soc.*, 1988, **110**, 244.
- 13 J. W. Walker, G. P. Reid, J. A. McCray and D. R. Trentham, *J. Am. Chem. Soc.*, 1988, **110**, 7170.
- 14 J. A. Mc Cray and D. R. Trentham, *Annu. Rev. Biophys. Biophys. Chem.*, 1989, **18**, 239.
- 15 V. S. Bannikov, *Biosens. Bioelectron.*, 1996, **11**, 933.
- 16 K. Tomizaki and H. Mihara, *J. Mater. Chem.*, 2005, **15**, 2732; I. Willner and E. Katz, *Angew. Chem.*, 2000, **112**, 1230; I. Willner and E. Katz, *Angew. Chem., Int. Ed.*, 2000, **39**, 1180; I. Willner, *Acc. Chem. Res.*, 1997, **30**, 347; I. Willner, A. Dagan, S. Rubin, R. Blonder, A. Riklin, Y. Cohen, *Eur. Pat. Appl.*, 1995, 47pp.
- 17 R. Heiligman-Rim, Y. Hirshberg and E. Fischer, *J. Phys. Chem.*, 1962, **66**, 2470.
- 18 C. Bohne, M. G. Fan, Z. J. Li, Y. C. Liang and J. Luszytk, *J. Photochem. Photobiol., A*, 1992, **66**, 79.
- 19 S. Delbaere, J. C. Micheau and G. Vermeersch, *Org. Lett.*, 2002, **4**, 3143.
- 20 A. Santiago and R. S. Becker, *J. Am. Chem. Soc.*, 1968, **90**, 3654.
- 21 M. Irie, K. Uchida, T. Eriguchi and H. Tsuzuki, *Chem. Lett.*, 1995, **24**, 899; M. Irie and M. Mohri, *J. Org. Chem.*, 1988, **53**, 803; S. Nakamura and M. Irie, *J. Org. Chem.*, 1988, **53**, 6136.
- 22 H. Kamogawa, M. Kato and H. Sugiyama, *J. Polym. Sci., Part A-1*, 1968, **6**, 2967; H. Rau, *Stud. Org. Chem.*, 1990, **40**, 165.
- 23 M. D. Cohen and G. M. J. Schmidt, *J. Phys. Chem.*, 1962, **66**, 2442; R. S. Becker and W. F. Richey, *J. Am. Chem. Soc.*, 1967, **89**, 1298.
- 24 D. Wöhrle, M. W. Tausch, W.-D. Stohrer, *Photochemie - Konzepte, Methoden, Experimente*, Wiley VCH, Weinheim, 1998, pp. 414–418.
- 25 A. Schmidt, M. Albrecht, T. Mordhorst, M. Topp and G. Jeschke, *J. Mater. Chem.*, 2007, **17**, 2793; A. Schmidt and M. Albrecht, *Z. Naturforsch.*, 2008, **63b**, 465; A. Schmidt, M. Topp, T. Mordhorst and O. Schneider, *Tetrahedron*, 2007, **63**, 1842; A. Schmidt, T. Mordhorst, H. Fleischhauer and G. Jeschke, *ARKIVOC*, 2005, **X**, 150.
- 26 A. Factor and G. Heinsohn, *J. Polym. Sci., Part B: Polym. Lett.*, 1971, **9**, 289.
- 27 M. S. Simon and P. T. Moore, *J. Polym. Sci., Polym. Chem. Ed.*, 1975, **13**, 1.
- 28 H. Kamogawa, H. Mizuno, Y. Todo and M. Nanasawa, *J. Polym. Sci., Polym. Chem. Ed.*, 1979, **17**, 3149; H. Kamogawa, T. Masui and M. Nanasawa, *Chem. Lett.*, 1980, **9**, 1145; H. Kamogawa, T. Masui and S. Amemiya, *J. Polym. Sci., Polym. Chem. Ed.*, 1984, **22**, 383; H. Kamogawa and S. Amemiya, *J. Polym. Sci., Polym. Chem. Ed.*, 1985, **23**, 2413; Kamogawa and S. Sato, *J. Polym. Sci., Part A: Polym. Chem.*, 1988, **26**, 653; Kamogawa, K. Kikushima and M. Nanasawa, *J. Polym. Sci., Part A: Polym. Chem.*, 1989, **27**, 393; Kamogawa and T. Ono, *Chem. Mater.*, 1991, **3**, 1020; H. Kamogawa and M. Nanasawa, *Bull. Chem. Soc. Jpn.*, 1993, **66**, 2443.
- 29 F. Neese, *Coord. Chem. Rev.*, 2009, **253**, 526.
- 30 Z. L. Madi, S. Van Doorslaer and A. Schweiger, *J. Magn. Reson.*, 2002, **154**, 181.
- 31 H. Kamogawa and T. Suzuki, *Bull. Chem. Soc. Jpn.*, 1987, **60**, 794.
- 32 J. Agejas, A. M. Cuadro, M. Pastor, J. J. Vaquero, J. L. Garcia-Navio and J. Alvarez-Builla, *Tetrahedron*, 1995, **51**, 12425.
- 33 X. Creary and H. Hartandi, *J. Phys. Org. Chem.*, 2001, **14**, 97.
- 34 C. Reichardt, *Solvents and Solvent Effects in Organic Chemistry*, Wiley VCH, 3rd edn, 2003.
- 35 A. R. Katritzky and B. Brycki, *J. Am. Chem. Soc.*, 1986, **108**, 7295.
- 36 A. L. Rieger and P. H. Rieger, *J. Phys. Chem.*, 1984, **88**, 5845.